Effect of confinement on statistical properties of a DNA chain in microchannels

Mauro Chinappi[1], Elisabetta De Angelis[2]
[1] *Dipartimento Meccanica e Aeronautica, Università di Roma "La Sapienza", via Eudossiana 18, 00184, Roma, Italia*
E-mail: mauro.chinappi@uniroma1.it

[2] *Dipartimento di Ingegneria delle Costruzioni Meccaniche, Nucleari, Aeronautiche e di Metallurgia- II Facoltà di Ingegneria, Università di Bologna, 47100 Forlì, Italia*

Keywords: mesoscale models, fluid dynamics, complex flows

SUMMARY. A particle-based mesoscopic model for fluid dynamics has recently introduced [14]. The model has been mainly developed for simulating a mesoscale coarse-grained dynamics for solvent-solute interaction in complex fluids such as polymers in solution and colloid suspension. In the present contribution the equilibrium properties and the relaxation dynamics of a DNA molecule are investigated. The model has proven to be fully able to capture the essential features of polymer dynamics in a good solvent. Moreover here this approach has been applied for the first time to study DNA dynamics in slit-like geometries.

1 INTRODUCTION

The alteration of the behavior of biopolymers, like DNA, in bounded geometry is observed in many circumstances both in nature or in technological applications. Let us think for instance to the recent development of micrifluidic devices designed for the manipulation of macromolecules. In such a scenario, a number of experimental and numerical studies have investigated relaxation dynamics of DNA in rectangular channels [10] while only recently some experimental investigation of DNA in slitlike geometry have appeared [3]. In this contribution we propose a numerical study of DNA relaxation in such a geometry. Actually the issue has been firstly studied by Brochard and de Gennes [5] that provide theoretical prediction for several statistical properties of polymer chains by means of the blob theory i.e. describing a polymer as a string of blobs of dimensions comparable with the confinement. Such theory obtains scaling laws for equilibrium extension of the polymer, center of mass diffusion and relaxation time.

The physics involved in such a setup accounts for a large number of degrees of freedom since in principle the range of time and length scales of the phenomena which affect the problem is large. Going from relaxation time of the chain and the microscale of the confining geometry to the rapid motions of the solvent molecules and the nanoscale of the interaction between those and the polymeric chain. In this perspective the problem is unfeasible for atomistic numerical simulation and a mesoscale description is needed.

The numerical results presented have been obtained simulating a modellized DNA molecule immersed in a solvent whose dynamics is coarse grained via a Multiparticle Collision Dynamic model [14], where only the slower time scale that can interact with the indolent motion of the DNA molecule are retained. Such a model is a particle based Navier Stokes solver introduced by Malevanets and Kapral [14]. In such approach both the Brownian dynamics and the hydrodynamic interaction are naturally accounted by the solvent model. Also the DNA molecule is modelled via a mesoscopic approach as a necklace of beads connected by wormlike chain springs, representing

the entropic elasticity associated with the stretching of one portion of the polymer, which interact via an excluded volume potential. The simulated system is a slit-like channel where the distance h between the walls is changed around values of the same order of magnitude of the equilibrium length of the DNA molecule. A stretched chain is positioned in the center of the channel and the relaxation towards equilibrium is studied. The effect of confinement it is expected to modify the dynamics of the polymer when the transversal dimension of the coil becomes of the same order of h.

The paper is structured as follows. A first section introduces the details of the simulations describing the model for the solvent and for the polymer. A second section goes through the results obtained both for confined and unconfined simulations. The formed are aimed to check the capability of the mesoscopic model to reproduce relevant characteristics of polymer dynamics. The latter simulations will show the dependency of the results on the different slit height.

2 MATHEMATICAL MODEL

2.1 *Solvent dynamics*

For the solvent modelling the multi particle collision dynamics [14] (MPCD, also known as stochastic rotation particle) approach is used. In MPCD the solvent is modelled as a system of N particles of mass m, position $\mathbf{x}_i$ and velocity $\mathbf{v}_i$, $i = 1, \ldots, N$. The time is discretized in interval of length Δt. The evolution of the system through a single time interval Δt is the result of two steps, namely the streaming and the collision steps. In the streaming step the particles dynamic is rules by standard Newton second law. The solvent particles don't interact with each other, hence, in absence of external forcing, the evolution is simply,

$$\mathbf{x}_i(t + \Delta t) = \mathbf{x}_i(t) + \Delta t \mathbf{v}_i(t). \tag{1}$$

In the collision step the system is divided in cubic cell of side l. For each cell c the mean velocity $\mathbf{V}_c$ is calculated as the average of instantaneous velocity of the particle inside the cell. The particle velocity is then changed according to

$$\mathbf{v}_i^a = \mathbf{V}_c + \omega \left(\mathbf{v}_i^b - \mathbf{V}_c \right) \tag{2}$$

where the apices a and b stand for "after" and "before" collision, while ω is a random rotation matrix. In this study we use a rotation of a fixed angle $\alpha = 5/6\pi$ in a uniformly distributed random direction. From the particle dynamics the solvent temperature is defined as $\theta = \langle m_i \mathbf{v}_i^2 \rangle / 3$, where we consider the Boltzmann constant equal to unit. Several theoretical and numerical studies analyzed the properties of MPCD solvent. In particular MPCD is able to reproduce in average the hydrodynamic motion [14, 13] The transport coefficient, such as viscosity, could be estimated as a function of statistic property of random matrix and fluid property (density, temperature, particle mass) [12, 9]. An additional step is implemented to ensure Galilean invariance [8], namely the grid defining the collision cells is shifted before each collision by a random vector whose component are extracted from a uniform distribution on the $[-l/2, l/2]$ interval. In the present study we used the length of the MPCD cell l as length unit, the mass m of a solvent particle as mass unit and $k_b\theta$ as energy unit.

2.2 *Polymer dynamics*

To model in a realistic way a polymer in a dilute solution both excluded volume and hydrodynamic interaction have to be taken into account. The polymeric chain is divided into segments each of them represening a subset of monomers and modelled by a bead and a spring. With such a choice the description of physical short-range interactions is neglected to achieve a feasible model

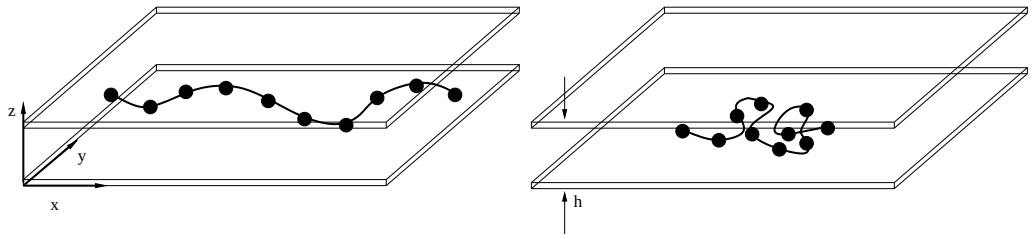

Figure 1: Sketch of domain representing the slitlike domain. Periodic boundary condition are applied in x and y directions. At the beginning of the simulation (left) the polymer is stretched along x direction, after a transient a coiled conformation is reached (right).

for long-range motions. More in detail our polymer is modelled, following [11], as a sequence of N_b bead of mass M whose position are indicated as $\mathbf{R}_i$. Adjacent beads interact by means of the spring potential

$$V_{ij}^s = \frac{k_b\theta}{2b_k}\left[R_0\left(1-\frac{R_{ij}}{R_0}\right)^{-1} - R_{ij} + \frac{2R_{ij}^2}{R_0}\right], \tag{3}$$

and the corresponding force

$$\mathbf{F}_{ij}^s = \frac{k_b\theta}{2b_k}\left[\left(1-\frac{R_{ij}}{R_0}\right)^{-2} - 1 + \frac{4R_{ij}}{R_0}\right]\frac{\mathbf{R}_{ij}}{R_{ij}}, \tag{4}$$

with b_k Kuhn length and $\mathbf{R}_{ij} = \mathbf{R}_i - \mathbf{R}_j$. Being N_k the number of Kuhn segments in the whole molecule, $N_{k,s}$ the number of segments in each of the spring and $N_s = N_b - 1$ the number of spring, we have $R_0 = N_{k,s}b_k$ and the total contour length of the polymer $L = N_k b_k = R_0 N_s$. The excluded volume interaction between all the beads pairs is

$$U_{ij}^{ev} = \frac{1}{2}vk_b\theta N_{k,s}^2\left(\frac{3}{4\pi S_s^2}\right)^{3/2}\exp\left[\frac{-3R_{ij}}{4S_s^2}\right] \tag{5}$$

with

$$S_s^2 = N_{k,s}\frac{b_k^2}{6} \tag{6}$$

and v the excluded volume parameter. In the overcited unit the mass of a single bead is, $M = 10$, $b_k 0.14$, $N_{k,s} = 17.4$ and $v = 0.012$. The beads do participate to the collision phase. Equations of motion for the beads are numerically integrated using a standard velocity Verlet scheme [2] with time step $\delta t = 0.1\Delta t$.

2.3 Confined simulations setup

We performed simulation in slitlike geometry with the two walls parallel to the Oxy plane, the z coordinate of the wall is indicated as z_w. In the streaming phase standard bounce back role [4] is applied to solvent particle. The polymer confinement is obtained with the repulsive LJ potential ($\sigma_w = 1$ and $\epsilon_w = 1$)

$$V(z_i) = 4\epsilon_w\left[\left(\frac{\sigma_w}{z_i - z_w'}\right)^{12} - \left(\frac{\sigma_w}{z_i - z_w'}\right)^{6}\right] + \epsilon_w \quad , \quad z_i - z_w' < 2^{1/6}\sigma_w \tag{7}$$

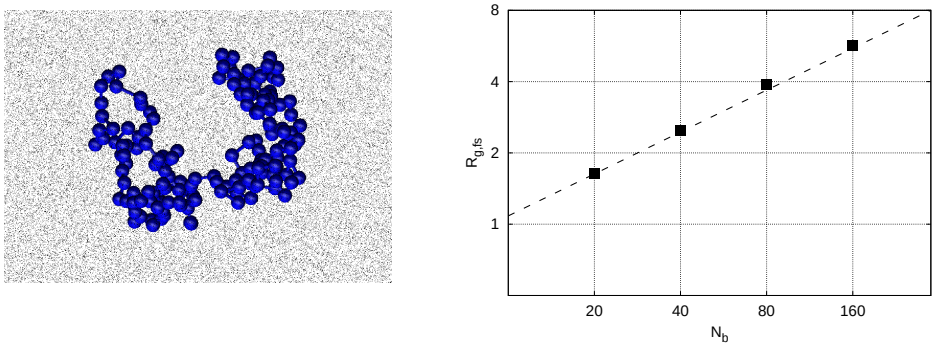

Figure 2: Left: Snapshot of a DNA modelled chain for $N_b = 160$ immersed in the mesoscopic solvent. Right: Gyration radius ($R_{g,fs}$) with respect to the number of beads N_b. The symbols represent the results of the numerical simulations while the dashed line is the theoretical prediction for the Zimm model for a good solvent.

and zero for $(z_i - z'_w) > 2^{1/6}\sigma_w$ acting on each bead. In expression 7 z_i is the bead z coordinate and z'_w is a plane placed at a distance σ_w inside the wall position (i.e. the $z = z_w$ plane at which bounce back is performed for solvent particles). Actually with this choise a bead at the wall ($z_i = z_w$) experienced a potential of θk_b hence, due to the stiffness of LJ potential the beads hardly cross the wall. On the other hand the LJ potential affect only a small slab $(2^{1/6} - 1)\sigma_w \simeq 0.12l$ thick, close to the wall resulting in the fact that the polymer is able to explore the whole channel. Concerning the collision phase we follow the implementation of Lamura et al. [13], where virtual thermalized particles were added to the collision cells crossed by the wall.

3 RESULTS

3.1 Unconfined simulations

In order to test our model some unconfined simulation (i.e. in a free space) have been performed at different molecular weights, namely $N_b = 20, 40, 80, 160$. Each molecule has been placed in a cubic box with periodic boundary conditions whose length size was approximately ten times the expected equilibrium stretch. Long simulations without any forcing have been performed and some relevant statistical observables have been collected. The first observable analyzed is the gyration radius $R_{g,fs}$ (where fs stays for free space), defined as [7]

$$R^2_{g,fs} = \frac{1}{N_b}\sum_{i=1}^{N_b}\langle(\mathbf{R}_i - \mathbf{R}_G)^2\rangle$$

with $\mathbf{R}_G$ is the position of the center of mass of the chain and $\mathbf{R}_i$ the beads positions. In the right panel of figure 2.3 its scaling behavior is reported as a function of the molecular weight, the results show a good agreement with the theoretical expectation

$$R_{g,fs} \simeq N_b^{\nu}, \tag{8}$$

where $\nu = 0.588$ for a long chain with excluded volume, i.e. Zimm model for a good solvent.

To evaluate the relaxation behavior of the DNA molecule, a Rouse normal coordinates analysis

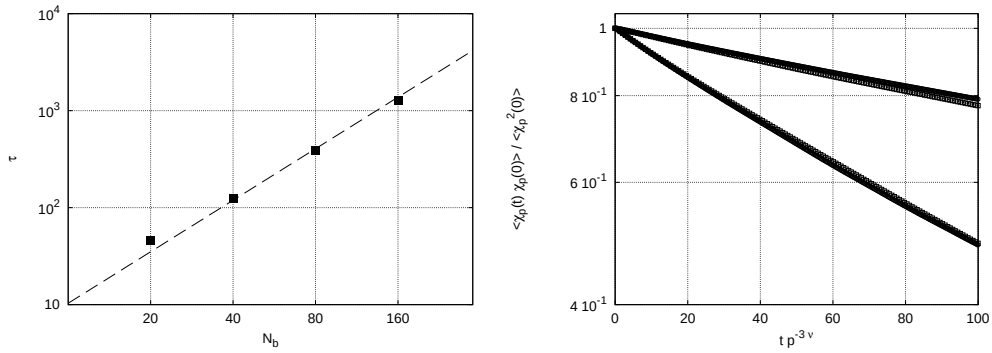

Figure 3: Left: Autocorrelation time of the first Rouse mode ($\tau_1 = \tau$) with respect to the number of beads N_b. The symbols represent the results of the numerical simulations while the dashed line is the theoretical prediction for the Zimm model for a good solvent. Right: Normalized autocorrelation for the first three Rouse modes rescaled with the respective theoretical predictions for $N_b = 40, 80$.

has been been performed. Defining the Rouse modes in their discrete version, as in [15],

$$\mathbf{X}_p = \frac{1}{N_b} \sum_{i=1}^{n} \mathbf{R}_i \cos\left[\frac{p\pi}{N}\left(i - \frac{1}{2}\right)\right] , \tag{9}$$

it is expected that the autocorrelation of the modes decays exponentially

$$\langle \mathbf{X}_p(t + t_0)\mathbf{X}_p(t_0)\rangle = \langle \mathbf{X}_p^2\rangle \exp\left(-\frac{t}{\tau_p}\right), \tag{10}$$

a theoretical prediction for the values of the relaxation times for the Rouse model can be given as [15]

$$\tau_p = \left(\frac{p}{N_b}\right)^{1/2} \sin^{-2}\left(\frac{p\pi}{N_b}\right). \tag{11}$$

Evaluating the l.h.s. of equation (10) for $p = 1$ allows for the identification of the longest relaxation time $\tau_1 = \tau$ for all the analyzed molecular weights. In figure 3 the behavior of τ against N_b is shown and once more a good agreement with the Zimm scaling in a good solvent, i.e. $\tau \sim N^{3\nu}$, is produced. For one (two) of the studied molecular weights, namely $N_b = 40$, the behavior of the normalized autocorrelation function (10) of the first three Rouse modes $\mathbf{X}_p$ is studied and the obtained time decay, showing a good exponential fit, is reported in figure 3. The x-axis has been rescaled for each relaxation time with the expected scaling behavior, $\tau_p \sim p^{-3\nu}$ [1]. The excellent agreement at least for the early stages of relaxation, without need of the correction proposed in [1], should be noted.

3.2 Confined simulations

The relaxation dynamics of DNA is studied via non equilibrium runs in which the DNA molecule, initially in elongated conformation along the x direction, spontaneously coils (fig. 1) up until it reaches an equilibrium configuration. Independent randomly generated configurations, where the polymer elongation in x direction was about 60% of the polymer contour length L_c, were used as initial conditions for the runs.

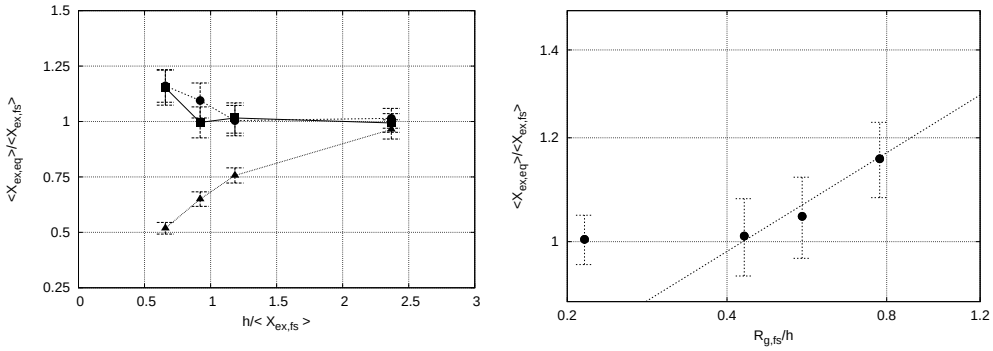

Figure 4: Left: Average polymer extensions (triangles $\langle Z_{eq} \rangle$, square $\langle Y_{eq} \rangle$, circle $\langle X_{eq} \rangle$) as functions of the channel height. All quantities are normalized with free space average extension. Right: Normalized wall parallel polymer extension plotted as a function of the inverse normalized channel height. The dashed line is the scaling prediction 12.

The statistic of the conformation of a coiled polymer in free space is isotropic. Hence, defined the free space polymer extension in x direction as $X_{ex,fs} = \max_x (x_1, \ldots, x_{N_b}) - \min_x (x_1, \ldots, x_{N_b})$, i.e. the length of the projection of the polymer on the x axis, and the analogous extensions Y_{ex} and Z_{ex} in the y and z directions respectively, the isotropy in free space implies $\langle X_{ex,fs} \rangle = \langle Y_{ex,fs} \rangle = \langle Z_{ex,fs} \rangle$. This is not the case in slitlike geometry, actually if the channel height h is comparable, or smaller, than $\langle Z_{eq,fs} \rangle$ confinement breaks isotropy and as reported by Balducci et al. [3] other alterations of the dynamical behavior set in.

Figure 4 reports the average values of a $N_b = 80$ polymer extensions in all the three direction as functions of channel height h ($h = 5, 7, 9, 18$). Both quantities are normalized with free space average extension. It is apparent that while for strong confinement – $h < \langle X_{ex,fs} \rangle$ – the z extension is smaller than free space one, while x and y extensions are slightly larger, for $h > 2\langle X_{ex,fs} \rangle$ the isotropy is fully recovered.

According to de Gennes the behavior of a linear polymer with persistence length b_k and contour length $N_k b_k$ confined in a slitlike channel with height h between the equilibrium length and b_k can be described as follows. The molecule is seen as a chain of blobs of dimension h, whose configuration follows a two-dimensional self-avoiding walk and no hydrodynamic interaction (HI) is assumed. The segments of the chain inside the blob follows a three-dimensional self-avoiding walk and they interact hydrodynamically. Under these assumptions, we obtain a scaling for the equilibrium extension with respect to height h as

$$\frac{\langle X_{ex,eq} \rangle}{R_{g,fs}} \sim \left(\frac{R_{g,fs}}{h} \right)^{1/4} \tag{12}$$

where the values of the exponents have been obtained using the ideal values $3/4$ e $3/5$ for the Flory-Edwards exponents ν_{2D} and ν_{3D} respectively. As shown in the right plot of figure 4, in our set-up the cross-over between free-space behavior to confined slit-like one occurs for values of $R_{g,fs}/h$ larger than 0.4 i.e. for approximately the same confinement as those reported in [6]. This plot shows that only two of our results seems to lay in a really confined regime, in any case the comparison with the expected scaling regime 12 is good.

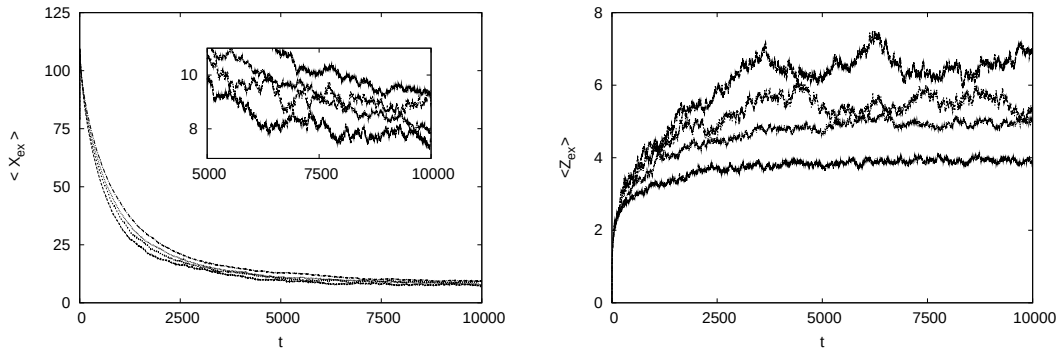

Figure 5: Left panel, time evolution of averaged extension $\langle X_{ex} \rangle$ of a $N_b = 80$ chain, the four curves correspond to $h = 5, 7, 9, 18$, the smaller channel corresponding to slower decaying to equilibrium values. The inset evidences that the asymptotic value is different. Right panel, time evolution of $\langle Z_{ex} \rangle$ for the same sets of simulations.

Ensemble average estimated on at least 50 independent simulations for each channel height, are calculated for time evolution of polymer extension. Left panel of figure 5 reports the time evolution of the ensemble average of extension X_{ex}. The four lines corresponds to the four channel heights and converge to the equilibrium values, being the slower one associated with the narrower channel. The inset clearly shows that the four asymptotic values are different as expected from equilibrium run (figure 4). The time evolution of $\langle Z_{ex} \rangle$ is reported right panel of figure 5. Here the difference among curves are more apparent, actually the smaller channel curves converge to a smaller value of Z_{ex} and the fluctuations around this values are much more dumped respect less confined cases. In particular once the regime values is reached ($t > 5000$) the $h = 5$ and $h = 7$ extension are more or less constant. This behavior is apparent also in a single realization (data not shown). On the other end for $h = 9$ and $h = 18$ the curves are much more rough. This effect, due to relatively poor statistics (only 50 simulations are used for ensemble average) is related to an higher equilibrium value of extension variance $\langle Z^2_{ex,eq} \rangle$ (for the four channel height from the smaller to the higher we have $\langle Z^2_{ex,eq} \rangle = 0.26, 0.80, 1.38, 5.49$). This effect is due to the fact that for channel smaller than free space extension the movement of the polymer are much more influenced by the confinement.

In order to better evidence the characteristics of the relaxation dynamics at different channel height, following Balducci et al. [3] we report in figure 6 the scaled squared extension along x direction defined as $\langle (X^2_{ex} \rangle - \langle X^2_{ex,eq} \rangle)/L^2_c$. In this figure the time is set to zero when the polymer extension is 30% of contour length ($\langle X_{ex}/L_c \rangle = 0.3$). A sort of double regime (fast relaxation for $t < 1500$ and slow relaxation near equilibrium, $2000 < t < 4000$) is observed. However it should be noted that the tail of the curves $2000 < t < 4000$ is dramatically affected by small changes in the value of $\langle X^2_{ex,eq} \rangle$. This could be easily explained in terms of error propagation, actually the relative error of scaled squared extension is proportional to the relative error in estimation of $\langle X^2_{ex,eq} \rangle$ with a factor of $\langle X^2_{ex,eq} \rangle / (\langle X^2_{ex} \rangle - \langle X^2_{ex,eq} \rangle)$. Near equilibrium this factor is very large, actually for $\langle X^2_{ex} \rangle = 1.1 \langle X^2_{ex,eq} \rangle$, obtained for $t \simeq 5000$ the factor is 10. Our accuracy in the determination of $\langle X^2_{ex,eq} \rangle$ do not allow us corroborate or not the two scaling law picture proposed by Balducci et al. [3], hence we concentrate our attention on the far from equilibrium relaxation dynamics ($t < 1000$).

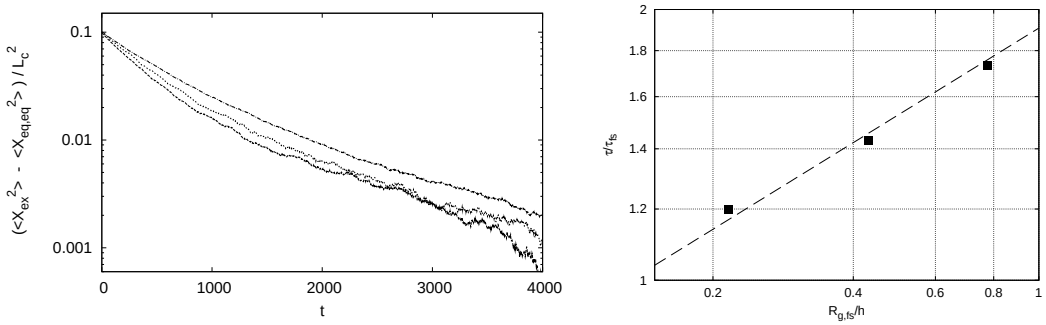

Figure 6: Left: Time evolution of scaled squared extension $(\langle X_{ex}^2\rangle - \langle X_{ex,eq}^2\rangle)/L_c^2$ for relaxation dynamics of a $N_b = 80$ polymer in three different channel ($h = 5, 9, 18$). The smaller the channel the slower the relaxation to equilibrium value. Right: Relaxation time far from equilibrium normalized with the bulk relaxation time versus normalized inverse channel height (symbols). The dashed line represent an empirical fit with slope 0.32.

Though confinement effects are still not strong in this regime when compared to [3] it is i still possible to observe a mild change in the relaxation dynamics. Actually the scaling of the altered relaxation time far from equilibrium shows a dependence on the channel height h which is weaker (h^{-32} vs. $h^{-0.5}$ than the one observed by [3], see right plot in figure 6. These results together with those in figure 4 corroborate the fact that our current simulations are in a mild confinement regime and further analysis for smaller channel heights might be useful.

4 CONCLUSIONS

The dynamics of a DNA chain both in unconfined and in a slitlike channel has been studied numerically via a novel mesoscopic approach. Results for the unconfined geometry show that the present numerical model is fully able to capture the essential features of polymer dynamics in a good solvent. Moreover, this approach has been applied for the first time to study DNA dynamics in slit-like geometries. Though the present analysis deals to mild confinement the present methodology appears to be an excellent candidate to reproduce and confirm recent results obtained in confined flow [3] and to test the results against existing theories.

ACKNOWLEDGEMENTS

We would like to thank Professor G. Graziani for the useful discussions. Simulations were in part performed on computing resources made available by CASPUR under HPC Grant 2009.

References

[1] P. Ahlrichs and B. Dünweg. Simulation of a single polymer chain in solution by combining lattice Boltzmann and molecular dynamics. *The Journal of Chemical Physics*, 111:8225, 1999.

[2] MP Allen and DJ Tildesley. *Computer Simulation of Liquids*. Oxford University Press, 1987.

[3] A. Balducci, C.C. Hsieh, and PS Doyle. Relaxation of Stretched DNA in Slitlike Confinement. *Physical Review Letters*, 99(23):238102, 2007.

[4] A. Berkenbos and C.P. Lowe. Accurate method for including solid-fluid boundary interactions in mesoscopic model fluids. *Journal of Computational Physics*, (227):4589–4599, 2008.

[5] F. Brochard and PG De Gennes. Dynamical scaling for polymers in theta solvents. *Macromolecules*, 10(5):1157–1161, 1977.

[6] Y.L. Chen, MD Graham, JJ de Pablo, GC Randall, M. Gupta, and PS Doyle. Conformation and dynamics of single DNA molecules in parallel-plate slit microchannels. *Physical Review E*, 70(6):60901, 2004.

[7] M. Doi and S.F. Edwards. *The Theory of Polymer Dynamics*. Oxford University Press, 1986.

[8] T. Ihle and DM Kroll. Stochastic rotation dynamics: A Galilean-invariant mesoscopic model for fluid flow. *Physical Review E*, 63(2):20201, 2001.

[9] T. Ihle, E. Tüzel, and DM Kroll. Equilibrium calculation of transport coefficients for a fluid-particle model. *Physical Review E*, 72(4):46707, 2005.

[10] R. M. Jendrejack, E. T. Dimalanta, D. C. Schwartz, M. D. Graham, and J. J. de Pablo. Dna dynamics in a microchannel. *Phys. Rev. Lett.*, 91(3):038102, Jul 2003.

[11] R.M. Jendrejack, J.J. de Pablo, and M.D. Graham. Stochastic simulations of DNA in flow: Dynamics and the effects of hydrodynamic interactions. *The Journal of Chemical Physics*, 116:7752, 2002.

[12] N. Kikuchi, CM Pooley, JF Ryder, and JM Yeomans. Transport coefficients of a mesoscopic fluid dynamics model. *Arxiv preprint cond-mat/0302451*, 2003.

[13] A. Lamura, G. Gompper, T. Ihle, and DM Kroll. Multi-particle collision dynamics: Flow around a circular and a square cylinder. *Europhysics Letters*, 56(3):319–325, 2001.

[14] A. Malevanets and R. Kapral. Mesoscopic model for solvent dynamic. *The Journal of chemical physics*, 110(17):8605–8613, 1999.

[15] M. Ripoll, K. Mussawisade, RG Winkler, and G. Gompper. Low-Reynolds-number hydrodynamics of complex fluids by multi-particle-collision dynamics. *Europhysics Letters*, 68(1):106–112, 2004.